

Design of Reactor—Separator—Recycle Systems Based on the Optimization of Estimations of the Domain of Attraction

Luis G. Matallana, Aníbal M. Blanco, and J. Alberto Bandoni*

PLAPIQUI (UNS-CONICET) Camino “La Carrindanga”, km. 7, (8000) Bahía Blanca, Argentina

ABSTRACT: In this paper, an optimization-based methodology is applied to the design of a reactor—separator—recycle system based on a measure of the extension of the domain of attraction of the operating equilibrium. The approach consists in maximizing the radius of a ball in the state space contained in the region of negative definiteness of the time derivative of a quadratic Lyapunov function. A two-level optimization strategy is proposed that solves a deterministic nonconvex global optimization problem at the inner level. To cope with the non-differentiability introduced by the inner problem, we applied a stochastic algorithm to manipulate the design variables at the outer level.

1. INTRODUCTION

Because of their outstanding importance in chemical and biochemical engineering, reacting systems have received very much attention from a nonlinear dynamics perspective in the last decades. Many studies have been presented on continuous stirred and tubular reactors in order to investigate their dynamics, from asymptotic stability to chaotic behavior. Most of the studies are based on simulation and bifurcation theory approaches. More recently, reactor—separator—recycle systems (RSRS) have also been addressed because of their unique open loop and closed loop nonlinear behavior.^{1–4}

Although the estimation of the domains of attraction of single reactors has motivated several studies,^{5–7} according to the best of our knowledge, no contributions on the analysis of the stability region of integrated RSRS have been presented so far.

The domain of attraction (DOA) or region of asymptotic stability of an asymptotically stable equilibrium point of a dynamic system is the portion of the state space where trajectories that converge to such equilibrium point originate. Some knowledge of its size and shape is usually required for the proper design and operation of the system.⁸ From a practical point of view, the extension of the DOA can be related to the robustness of the dynamic system to restore its original operating condition once the disturbances that altered its steady-state condition are removed.

For the general case, however, the DOAs of equilibrium points of general nonlinear systems are complicated sets that do not admit analytical representation.

While the estimation of the DOA of a given asymptotically stable equilibrium has been largely addressed, the design of the nonlinear system with a specific focus on the extension of the DOA has been less studied. This is indeed a challenging problem because it is related to other two important underlying problems: the “design-for-stability-problem” and the “DOA estimation problem”.

The design-for-stability problem essentially seeks to find an operating equilibrium point which is asymptotically stable while optimizing some appropriate objective function, typically economical. Such an important problem has been addressed with different approaches in many disciplines. In Kokossis and

Floudas,⁹ an iterative strategy to bound the eigenvalues of the Jacobian matrix was applied to the synthesis of reactor networks. In Ringertz,¹⁰ different problems of the mechanical engineering discipline were addressed through an eigenvalue optimization technique that relies on an interior point/logarithmic barrier transformation approach. Monningmann and Marquardt,¹¹ presented a steady-state design methodology which addressed the robust stability issue making use of bifurcation theory elements. The proposed approach was applied to a continuous polymerization process in that work, to the notable HDA process in Monningmann and Marquardt¹² and to a biosynthesis model in Gerhard et al.¹³ In Blanco and Bandoni,¹⁴ eigenvalue optimization techniques, which make use of standard NLP solvers to constrain the real part of the eigenvalues were described, and applied in Matallana et al.¹⁵ to a fermentation process. In Chang and Sahinidis,¹⁶ the design under stability problem was formulated as a bilevel optimization problem and its solution addressed with global optimization algorithms. The approach was illustrated through several metabolic pathways of different complexity. More recently, in Lu et al.,¹⁷ the robust stability design problem was addressed as an eigenvalue assignment problem. A stochastic algorithm was adopted in that work to solve the resulting nonconvex, nondifferentiable optimization problem. The common framework of the above-described work is the optimization of a certain “cost” objective function while guaranteeing local dynamic asymptotic stability of the equilibrium at the solution.

Regarding the estimation of DOAs, many techniques have been proposed so far. The interested reader is referred to Genesio et al.¹⁸ for a clear classification of the techniques and a review of classic work on the topic. In particular, the Lyapunov stability theory provides a methodology whose rationale is to approximate the DOA by a level set of a Lyapunov function. Usually, polynomial type Lyapunov functions are adopted. Basically, the idea is to find the largest level set of the Lyapunov

Received: November 17, 2010

Accepted: April 19, 2011

Revised: April 4, 2011

Published: April 19, 2011

function fully contained in the region of negative definiteness of its time derivative.

Recently, a design problem was proposed in order to find an asymptotically stable equilibrium point whose DOA is the largest in some sense.¹⁹ The estimation of DOAs based on appropriate level sets of Lyapunov functions were adopted, while the stability issue was addressed by forcing the eigenvalues of the Jacobean matrix of the dynamic system to belong to the left half of the complex space. A two level optimization approach was proposed to solve the resulting “bi-level” optimization problem.

In this contribution, such methodology is applied to the design of the important RSRS. The remainder of the paper is organized as follow. Section 2 introduces basic definitions and theorems used along the paper. In section 3, the design formulation based on the optimization of the DOA is presented. In section 4, the RSRS is described. In section 5, the design methodology is applied to the system under study. A conclusions section closes the paper.

2. BACKGROUND DEFINITIONS AND THEOREMS

In this section, the basic definitions and theorems required to support the proposed contribution are introduced. All of these can be found in classic texts on nonlinear systems analysis such as Khalil,⁸ Vidyasagar,²⁰ and Hahn.²¹

Consider the following autonomous nonlinear dynamic system

$$\frac{dx}{dt} = f(x), x \in \mathcal{R}^n, x(t_0) = x_0 \quad (1)$$

where $x = x^*$, an asymptotically stable equilibrium point of 1.

Definition 2.1. (Equilibrium point). A point $x^* \in \mathcal{R}^n$ is called an equilibrium point of system 1 if $f(x^*) = 0$. The equilibrium points of system 1 correspond the intersection of the null clines of the system, meaning the curves given by $f(x) = 0$.

Remark 2.1. In the sequel, we assume without loss of generality, that the equilibrium point under study coincides with the origin of the states space of \mathcal{R}^n , ($x^* = 0$).

Definition 2.2. (Asymptotic stability). Let $x(t, x_0)$ denote the trajectory initiated at state x_0 in time t_0 . Equilibrium $x^* = 0$ of system 1 is asymptotically stable if there exists a $\delta > 0$ such that: $\lim_{t \rightarrow \infty} x(t, x_0) = 0$, whenever $\|x_0\| < \delta$

Definition 2.3. (Positive and negative definite functions). A continuously differentiable real-valued function $\varphi(x)$ defined on a domain $R(0) \subseteq \mathcal{R}^n$ containing point $x = 0$ is called positive definite if the following conditions hold:

$$\varphi(0) = 0$$

$$\varphi(x) > 0 \quad \forall x \in \{R(0) \setminus 0\}$$

Function $\varphi(x)$ is negative definite if $-\varphi(x)$ is positive definite.

Remark 2.2. In the remaining, the symbol >0 (<0) is used to denote positive (negative) definiteness of functions.

Lyapunov stability theory provides the basis of a family of techniques for estimation of regions of asymptotic stability whose rationale is to approximate the DOA(0) by a level set of a Lyapunov function of the equilibrium point.

Definition 2.4. (Lyapunov function). Let $V(x)$ be a continuously differentiable real-valued function defined on a domain $D \subseteq \mathcal{R}^n$ containing equilibrium $x = 0$. Function $V(x)$ is a Lyapunov function of equilibrium $x = 0$ of system 1 if the following conditions hold:

$V(x)$ is positive definite on $R(0)$

The time derivative of $V(x)$, $(dV(x))/(dt) = [\nabla V(x)]^T f(x)$, is negative definite on $R(0)$.

Theorem 2.1. (Asymptotic stability in the Lyapunov sense). If there exists a Lyapunov function $V(x)$ for equilibrium point $x = 0$ of system 1, then $x = x^* = 0$ is asymptotically stable.

Definition 2.5. (Domain of attraction). The DOA of the equilibrium point $x = 0$ is given by:

$$\text{DOA}(0) = \{x_0 \in \mathcal{R}^n : \lim_{t \rightarrow \infty} x(t, x_0) \rightarrow 0\} \quad (2)$$

Theorem 2.2. (Estimation of the domain of attraction). Let $V(x)$ be a Lyapunov function for equilibrium $x = 0$ of system 1. Consider that $dV(x)/dt$ is negative definite in the region

$$S(0) = \{x : V(x) \leq c, c > 0\} \quad (3)$$

Then, every trajectory initiated within region $S(0)$ tends to $x = 0$ as time tends to infinity.

Theorem 2.3. (Jacobian matrix spectrum). If equilibrium $x = 0$ of system 1 is exponentially stable, then the real part of the eigenvalues of the corresponding Jacobean matrix, A , are strictly negative.

Theorem 2.4. (Lyapunov identity). If equilibrium $x = 0$ of system 1 is asymptotically stable, then there exists a Lyapunov function of the quadratic type, $V(x) = x^T P x$, where P is a positive definite matrix that can be calculated from the so-called Lyapunov identity

$$A^T P + P A = -Q \quad (4)$$

where Q should required to be positive definite. A common choice is to set $Q = I$ where I is the identity matrix.

Theorem 2.5. Consider the following representation of system 1: $f(x) = Ax + f_1(x)$, where $f_1(x)$ comprises the nonlinear part of function $f(x)$. It can be shown²⁰ that if the following condition holds:

$$\frac{\|f_1(x)\|}{\|x\|} \leq \frac{\lambda_{\min}(Q)}{2\lambda_{\max}(P)}, \quad \forall x \in B_r \quad (5)$$

$V(x)$ and its time derivative are positive and negative definite, respectively, within the ball B_r of radius r . It is clear that the larger the ratio $\lambda_{\min}(Q)/2(\lambda_{\max}(P))$, the larger the possible choice of r .

3. DESIGN FORMULATION BASED ON THE OPTIMIZATION OF DOA ESTIMATIONS

If dynamic stability constraints are introduced in an economic design formulation, the resulting equilibrium point is guaranteed to possess a certain DOA. However, if no explicit consideration on the extension of such stability region is included, the operating equilibrium might lie close to some of its boundaries. If this is the case, even modest disturbances in certain directions might drive the state variables beyond such boundaries, preventing the system to return to the original steady state once the disturbances are removed. In this section, the methodology presented in Matallana et al.¹⁹ to account for extension of DOA estimates within the design problem is introduced. The interested reader is referred to the original paper for the details.

Whereas for the general case the DOA of a stable equilibrium is a set of complex shape and possible infinite size, estimations based on quadratic Lyapunov functions are always hyper-ellipses contained in the ball B_r previously defined in eq 5. The radius r of

- Step 1 - Generate an initial population for design variables [\mathbf{d} , \mathbf{x}_0]
- Step 2 - For each member of the population calculate the equilibrium \mathbf{x}_s
- Step 3 - Evaluate merit function r as follows
- If \mathbf{x}_s does not exist then set $r = 0$
 - If \mathbf{x}_s does exist then evaluate the eigenvalues of Jacobean matrix $\mathbf{A}(\mathbf{d}, \mathbf{x}_s)$
 - If the real part of some of the eigenvalues is positive then set $r = 0$
 - If the real part of all the eigenvalues is negative then solve problem (6c) to evaluate radius r
- Step 4 - Check the stopping criterion
- If the stopping criterion is not verified then generate a new population based on the value of the objective function of the individuals and return to Step 2.
 - If the stopping criterion is verified then terminate

Figure 1. Resolution procedure of problem 6.

such a ball is used in this work as a merit function for the design optimization problem.

The rationale behind such an approach is that the enlargement of the radius of the described ball has a “push away” effect on the actual boundaries of the DOA no matter their shape and localization. Such boundaries are usually the stable manifolds of saddle nodes and limit cycles. Moreover, an enlarged ball can be also obtained at the expense of a shift of the equilibrium in the state space. Therefore, the effect of seeking an optimized radius is a net increase in the actual region of asymptotic stability. The problem is stated as follows

$$\begin{aligned}
 &\max_{r, \mathbf{x}_s, \mathbf{d}} \quad r \\
 &s.t. \mathbf{f}(\mathbf{x}_s, \mathbf{d}) = \mathbf{0} \quad (a) \\
 &\text{Re}\{\lambda_i[\mathbf{A}(\mathbf{x}_s, \mathbf{d})]\} < 0 \quad i = 1, \dots, n \quad (b) \\
 &\left\{ \begin{array}{l} \min_{r, \mathbf{x}, \mathbf{P}} \quad r \\ s.t. \|\mathbf{x}\| - r = 0 \\ \mathbf{A}(\mathbf{x}_s)^T \mathbf{P} + \mathbf{P} \mathbf{A}(\mathbf{x}_s) = -\mathbf{I} \\ \frac{\|\mathbf{f}_1(\mathbf{x})\|}{\|\mathbf{x}\|} - \frac{1}{2\lambda_{\max}(\mathbf{P})} = 0 \\ r > 0 \end{array} \right\} \quad (c) \quad (6) \\
 &\mathbf{d}^L \leq \mathbf{d} \leq \mathbf{d}^U \\
 &\mathbf{x}^L \leq \mathbf{x} \leq \mathbf{x}^U
 \end{aligned}$$

Equation 6a is the dynamic system in steady state version. \mathbf{x}_s is the equilibrium point and \mathbf{d} is the vector of design variables.

Constraint 6b stands for the asymptotic stability constraint of the equilibrium point \mathbf{x}_s by imposing that the real part of the eigenvalues of the Jacobean matrix $\mathbf{A}(\mathbf{d}, \mathbf{x}_s)$ be strictly negative.

Constraint 6c is an optimization problem for the calculation of the radius of ball B_r . Variable r represents the distance between the stable equilibrium \mathbf{x}_s and the point in the states space, \mathbf{x} , where the surface of the ball B_r and the surface defined by $(\|\mathbf{f}_1(\mathbf{x})\|)/(\|\mathbf{x}\|) - (\lambda_{\min}(\mathbf{Q}))/2\lambda_{\max}(\mathbf{P}) = 0$ intersects. Constraint (6c) is an optimization problem itself, which has to be solved to global optimality because local solutions are not appropriate as thoroughly discussed in Matallana et al.^{19,22}

Because the real part of the eigenvalues of a matrix do not possess explicit expressions to be written down for the general case in 6b, and subproblem 6c does not admit an analytical

solution either, a two-level solution strategy was proposed to address problem 6.

In the “outer level” a stochastic “derivative free” optimization engine is adopted to explore the design variables space. The stochastic engine is based on the evolution of a population of solutions according to a set of rules. For each individual of the population of design variables, an equilibrium point \mathbf{x}_s is calculated from 6a and its feasibility with respect to constraint (6b) verified. If the equilibrium is asymptotically stable, problem 6c is solved at the “inner level” to find the ball which verifies 5 and its radius is returned as the objective function value to the stochastic optimizer. A deterministic solver is adopted at the “inner level”. In order to avoid issues introduced by steady state multiplicity, the design variables vector is enlarged with the starting point vector, \mathbf{x}_0 , for the Newton-type search adopted to solve system 6a. The pseudocode in Figure 1 summarizes the proposed procedure.

If no equilibriums exist or they are unstable, then no DOAs exist and their radiuses are set to zero (steps 3a and 3b-i). If stable equilibriums exist, their merit function assumes the actual value of the radiuses (step 3b-ii). In this way, stable equilibriums with the largest radiuses are favored in the search.

In this contribution, a standard implementation of a genetic algorithm is adopted.²³ It should be mentioned that a major drawback of stochastic solvers is the lack of a general technique for the handling of constraints other than upper and lower bounds on the variables. However, in this application not such constraints exist since the search space is only box constrained in problem 6 because constraints 6a–c are calculated in a sequential fashion (Figure 1).

It should be noted that 6c is a nonlinear optimization model and therefore it may have many local solutions. In order to avoid trivial solutions, problem 6c has to be solved to global optimality.^{19,22} Global optimality is ensured in this work by using state of the art global optimization software. In particular, the GAMS platform²⁴ with the global optimization solver BARON²⁵ is adopted. BARON implements a deterministic global optimization algorithm of the branch and bound type, which guarantees to provide the global optima under fairly general assumptions. For a complete presentation of the theory behind the BARON solver, see Tawarmalani and Sahinidis.²⁶

The main requirement of the BARON²⁵ solver is essentially the provision of appropriate lower and upper bounds for every variable and expression of the model. Regarding the type of nonlinearities, BARON can handle most nonlinear functions typically found in chemical engineering models, including multiplication, division, and exponentiation. Regarding the

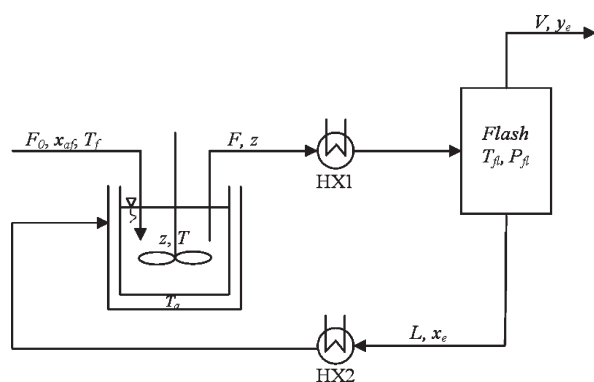


Figure 2. Schematic diagram of the RSRS.

architecture,²⁶ BARON implements a branch and bound algorithm with additional components (domain reduction, relaxation strategies, branching decisions, etc.). The computational performance²⁶ of the solver has been tested with various sets of nonlinear models. The overall conclusion is that computational requirements increase with problem size and are highly dependent on the type and number of nonlinearities present in the model as well as on the adopted formulation.

Experimental evidence with problem 6 indicates that the maximization of the radius of ball B_r “pushes away” the boundaries of the DOA which are close to the equilibrium under study. Moreover, a shift in the position of the equilibrium inward the stability region may also occur. These are indeed desired effects since the equilibrium point “moves away” the boundaries of the DOA, which translates into an effective “enlargement” of the region of stability. However, it should be emphasized that, in fact, an estimation of the DOA is being optimized rather than the actual region of stability. For simplicity “optimized DOA” is used in the following to refer to the solution corresponding to the optimized DOA estimation.

4. REACTOR–SEPARATOR–RECYCLE SYSTEM

In this section, the adopted RSRS is described (Figure 2). The model is an adapted version from the one presented in Vetukuri et al.,⁴ which was used in many articles to study different aspects of the nonlinear behavior of this type of systems. Fresh reactant A is fed (F_0, x_{af}) to the continuous stirred tank reactor where a first order exothermic reaction $A \rightarrow B$ takes place. The reaction mixture (F, z) enters a flash operated at constant pressure and temperature (T_{fl}, P_{fl}). The flash vapor stream (V, y_e), rich in product B, leaves the system, whereas the liquid stream (L, x_e), rich in reactant A, is recycled back to the reactor. It is assumed that the temperatures of the flash inlet and recycle streams can be perfectly controlled by means of heat exchangers (HX1, HX2).

It is assumed that the fresh flow-rate of reactant A, F_0 , is externally specified and that the reactor holdup is perfectly controlled by the reactor effluent flow-rate, F . In dimensionless fashion, the model equations for the integrated reactor-flash-recycle system are

$$\frac{dz}{dt} = x_{af} - y_e - D_{a1} z \exp(\theta) \quad (7)$$

$$\frac{d\theta}{dt} = -\theta \left[1 + \frac{(y_e - z)}{(z - x_e)} + \beta D_{a1} \right] + \beta D_{a1} z \exp(\theta) \quad (8)$$

Table 1. Model Parameters

parameter	description	value	units
F_0	feed flow rate	1.0	mol/seg
x_{af}	mole fraction of A in feed stream	1.0	
P_{fl}	flash pressure	101 325	Pa
k_0	preexponential factor	1.0×10^4	seg ⁻¹
E	activation energy	40 000	J/mol
R	gas constant	8.3144	J/(mol K)
C_{pm}	molar heat	209.836	J/(mol K)
T_f	feed temperature	298	K
T_a	refrigerant temperature	298	K
ρ_m	density	1200	mol/m ³
U	heat transfer coefficient	567.82	J/(seg m ² K)
Δh_A	heat of vaporization of A	38 331.15	J/mol
Δh_B	heat of vaporization of B	28 748.16	J/mol
A_A	Antoine constant	-21.4611	Pa
B_A	Antoine constant	-3974.04	K
A_B	Antoine constant	-26.0821	Pa
B_B	Antoine constant	-4366.82	K

where θ stands for dimensionless reactor temperature, B represents the dimensionless heat of reaction, β represents the dimensionless heat transfer coefficient in the reactor, and D_{a1} is the Damköhler number according to the following definitions

$$B = \frac{(-\Delta H)E}{(C_{pm}RT_f^2)}, \quad \beta = \frac{UA_r}{V_r k_0 \exp\left(\frac{-E}{RT_f}\right) C_{pm} \rho_m},$$

$$D_{a1} = \frac{V_r k_0 \exp\left(\frac{-E}{RT_f}\right) \rho_m}{F_0}, \quad \theta = \frac{E(T - T_f)}{RT_f^2}$$

Variable t stands for dimensionless time by scaling the time variable with the molar holdup to fresh feed ratio (M_r/F_0). The vapor–liquid equilibrium in the flash is described through relations 9–13, which relate the vapor and liquid compositions with the operating temperature and pressure of the unit. For the purposes of this study, the process is operated at atmospheric pressure (101 325 Pa). The parameters for this model are shown in Table 1.

$$y_e = K_A(T_{fl}, x_e) x_e \quad (9)$$

$$1 = K_A(T_{fl}, x_e) x_e + K_B(T_{fl}, x_e) (1 - x_e) \quad (10)$$

$$K_i = \frac{P_i^{\text{sat}} T_{fl}}{P} \quad i : A, B \quad \text{Ideal gas phase} \quad (11)$$

$$\ln\left(\frac{P_i^{\text{sat}}}{P}\right) = \left(\frac{\Delta h_i}{R}\right) \left(\frac{1}{T_i} - \frac{1}{T_{fl}}\right) \quad i : A, B \quad \text{Clasius – Clapeyron equation} \quad (12)$$

$$\ln(P) = A_i + \frac{B_i}{T_i} \quad i : A, B \quad \text{Antoine equation} \quad (13)$$

5. DESIGN STUDY

Two design studies are performed: (i) a classic design problem with an economic objective function and eigenvalue stability constraints and (ii) problem 6 as described in section 3.

The economic-based design problem 14 seeks to optimize a cost objective function while requiring dynamic asymptotic stability of the resulting operating equilibrium. Problem 14 is solved in this contribution using the GAMS/BARON platform. For this two-states system, constraint 14b on the real part of the eigenvalues is reformulated in terms of the trace and the determinant of matrix \mathbf{A} ,²⁷ leading to classic a NLP problem.

$$\begin{aligned} \min_{\mathbf{x}, \mathbf{d}} \quad & \phi \\ \text{s.t.} \quad & \mathbf{f}(\mathbf{x}_s, \mathbf{d}) = \mathbf{0} \quad (\text{a}) \\ & \text{Re}\{\lambda_i[\mathbf{A}(\mathbf{x}_s, \mathbf{d})]\} < 0 \quad i = 1, \dots, n \quad (\text{b}) \\ & \mathbf{d}^L \leq \mathbf{d} \leq \mathbf{d}^U \\ & \mathbf{x}^L \leq \mathbf{x} \leq \mathbf{x}^U \end{aligned} \quad (14)$$

For both problems, 6 and 14, the design optimization variables are the reactor volume, the flash drum volume and the areas of the heat exchangers HX1 and HX2 (V_r , V_{fl} , A_{HX1} and A_{HX2} , respectively). Because the objective of the RSRS is to produce component B, a product quality constraint is imposed on the product stream (vapor stream of the flash), by limiting the concentration of component A (y_e), to be within a small range.

The economic objective to be minimized in problem 14 is the capital cost of the process

$$\phi = \frac{1}{\beta_{\text{pay}}} (C_{\text{reactor}} + C_{\text{flash}} + C_{\text{exchangers}}) \quad (15)$$

where β_{pay} is the payback period (3 years) and C_{reactor} , C_{flash} and $C_{\text{exchangers}}$ are the costs of the individual units. The capital cost of the reactor depends on its size and is calculated as

$$C_{\text{reactor}} = 17639(D_r)^{1.066} + (2D_r)^{0.802} \quad (16)$$

where D_r is the reactor diameter in meters. Assuming that the height of the reactor is twice its diameter the relationship between the diameter and the volume is:

$$D_r = (0.6366V_r)^{1/3} \quad (17)$$

The heat transfer reactor area depends of the reactor diameter D_r according to the equation

$$A_r = 2\pi D_r^2 + \frac{\pi}{4} D_r^2 \quad (18)$$

The capital cost of the flash separator depends on its diameter, D_{fl} , according to 19

$$C_{\text{flash}} = 7308.26(D_{fl})^{1.066} + 548.8(D_{fl})^{1.55} \quad (19)$$

The diameter is affected by the incoming flow rate, through the following relation

$$D_{fl} = 3.9929 \left(\frac{F}{\rho_m} \right)^{1/3} \quad (20)$$

The capital cost of the heat exchangers depends on its heat exchange areas A_{HX1} and A_{HX2} , which are, in turn, related to the energy balances

$$C_{\text{exchangers}} = 8701(A_{HX1})^{0.65} + 8701(A_{HX2})^{0.65} \quad (21)$$

The energy balances in heat exchangers HX1 and HX2 are

Table 2. Data and Results for RSRS

$B = 14, F_0 = 1$	optimal cost (14)	optimal DOA (6)
D_r [0.5; 1.5]	0.6485	1.4157
y_e [0; 0.15]	0.15	0.1194
β	16.0595	7.3564
x_e	0.8283	0.7954
T_{fl}	348.35	343.5032
T	319.12	303.78
V_r	0.4283	4.4569
A_r	2.9726	14.1669
Da_1	0.5008	5.2112
D_{fl}	0.5048	0.3765
Q_{fl}	4.0687×10^4	3.8278×10^4
A_{HX1}	1.7365	3.5017
A_{HX2}	0.5807	0.0047
F	2.3562	1.0061
L	1.3562	0.0061
V	1.00	1.00
z_s	0.5404	0.1235
θ_s	1.1442	0.3133
$\lambda_{1s}(\mathbf{A})$	$-0.0366 + 2.8969i$	-13.6992
$\lambda_{2s}(\mathbf{A})$	$-0.0366 - 2.8969i$	-20.4433
$\lambda_{1s}(\mathbf{P})$	7.1696	0.0150
$\lambda_{2s}(\mathbf{P})$	140.9489	0.5711
cost	12.5154×10^3	27.1627×10^3
r	0.5307×10^{-2}	1.7393×10^{-2}

$$Q_{HX1} = V\Delta h - FC_{pm}(T - T_{fl}) = UA_{HX1}(\Delta T_{ml})_{HX1} \quad (22)$$

$$Q_{HX2} = LC_{pm}(T_{fl} - T) = UA_{HX2}(\Delta T_{ml})_{HX2} \quad (23)$$

where ΔT_{ml} is the logarithmic mean temperature for the heat exchangers. It is supposed that a large flow-rate of the service fluid is used in both cases such that its temperature, T_s , can be assumed constant for the calculations.

Table 2 presents the results of design problems 14 and 6 for the RSRS. The corresponding solutions are depicted on the state space in Figures 3 and 4.

In panels a and b in Figure 3 are shown the null clines of system 7–8 (solid and dashed lines) together with the actual DOAs of the operating equilibrium point (white regions). In panels a and b in Figure 4 are shown ball B_r (solid line) together with surface $(\|f_1(\mathbf{x})\|)/(\|\mathbf{x}\|) - (1)/(2\lambda_{\max}(\mathbf{P})) = 0$ (dashed line) in the deviation variables state ($x_1 = z - z_s$ and $x_2 = \theta - \theta_s$). It is also explicitly indicated the intersection point between both level sets.

By inspection of the cost variable in Table 2 and the comparison of panels a and b in Figure 3, it can be concluded that, as expected, model 14 provides a cheaper design, whereas model 6 generates a more robust one from the point of view of the extension of the DOA.

From Figure 3a, two equilibrium points in the state-space can be observed: the stable one and a saddle node. It is clear that the boundary of the DOA in this case is the stable manifold of the saddle. In the solution of problem 6 (Figure 3b), on the other hand, the boundary of the DOA is the region of the states space where the singularity of the denominator of eq 8 takes place. The

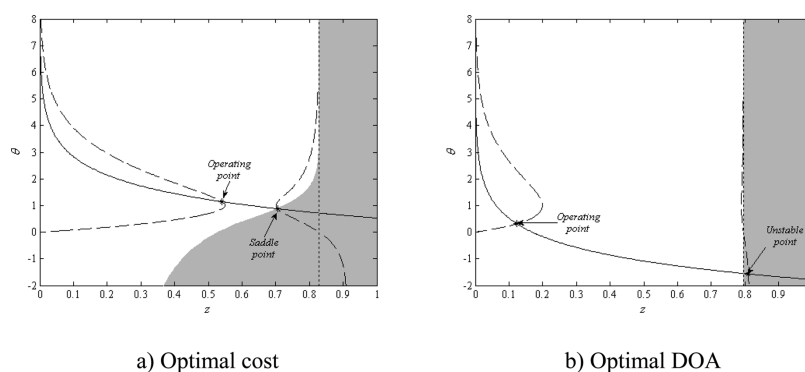


Figure 3. Null clines and actual DOA (white region).

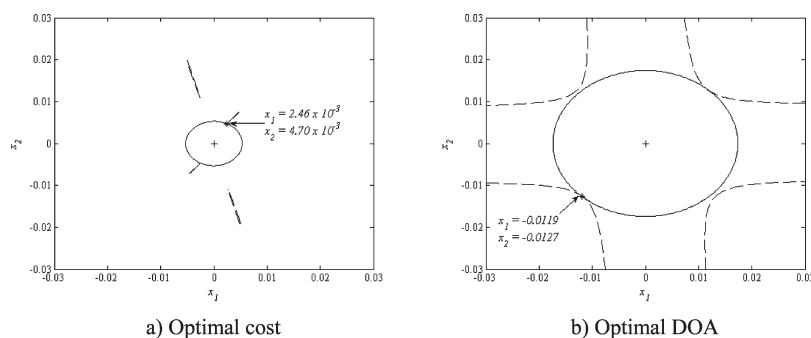


Figure 4. Ball B_r (solid), constraint 5 (dashed).

second equilibrium point is not a saddle anymore but an unstable node and lies beyond the boundary. Evidently a significant change in the topology of the system has occurred as result of the optimization.

It can be observed that a significant increase in the DOA regarding the one of the economic design has taken place. Such an enlargement has to do with the optimization of the size of ball B_r . It can be seen that the radius of the ball B_r is sensibly enlarged in Figure 4b regarding the one of Figure 4a, as expected. Besides the enlargement of this DOA related measurement, there has also been a significant shift of the operating equilibrium point between both solutions.

As a general conclusion it can be noted the conflicting nature between the economic and the operability objectives. In this case, operability is related to the extension of the stability region. A larger stability region (Figure 3b) can be obtained at the expense a worse economic objective function value. This trade-off between economics and operability of chemical processes has been extensively acknowledged by the process systems engineering community in the last years.^{28–31}

From a physical point of view, the reactor corresponding to the optimal economic design is much smaller than the one resulting from the optimized DOA. Therefore, although the reactor works at a relatively high temperature level, its conversion is low. For this reason larger internal flow-rates (F and L) have to be processed, increasing the required size of the heat exchangers and flash drum. However, the reduced cost of a small reactor compensates the large costs of the other units.

Because the reactor of the optimal DOA design is larger than its economically optimal counterpart, the downstream equipment

is therefore less expensive, because a large conversion takes place in the reaction step and a small recycle is required.

The relationship between the extension of the DOA and the levels of the design variables at the solution is not obvious due to the presence of complex nonlinearities in the balance equations. However, it is clear for example, that the reaction temperature produces a large effect on the system because it is amplified by the exponential terms of eqs 7 and 8. The small reactor volume in the optimal economic design requires a relatively high reaction temperature to achieve a significant conversion. On the other hand, the larger reactor of the DOA optimized design converts enough at a lower temperature level. At low temperatures and conversions, the system operates far from the boundaries of the DOA, making the process more robust to disturbances.

It can be also observed from Table 2 that the real part of the eigenvalues is close to the imaginary axis for the economically optimal design, whereas they are deep inside the stable hyperplane for the DOA optimized design. The magnitude of these figures provides an intuitive measure of the robustness of the system regarding asymptotic stability. If the real part of the eigenvalues of the original operating point are relatively large in absolute value, the system is far from a bifurcation point. Therefore, in the face of a small disturbance on some of the parameters, the new steady state is likely to remain stable.

To illustrate the practical effect of an enlarged DOA, the operation for both process designs is disturbed with a step in the feed temperature T_f from 298 to 290 K. After a lapse of 0.5 (dimensionless time), temperature T_f is restored to its original level. The results of the simulation are shown in Figure 5. In Figure 5a, it can be observed that for the optimal cost design, the trajectory has left the DOA of the operating equilibrium after

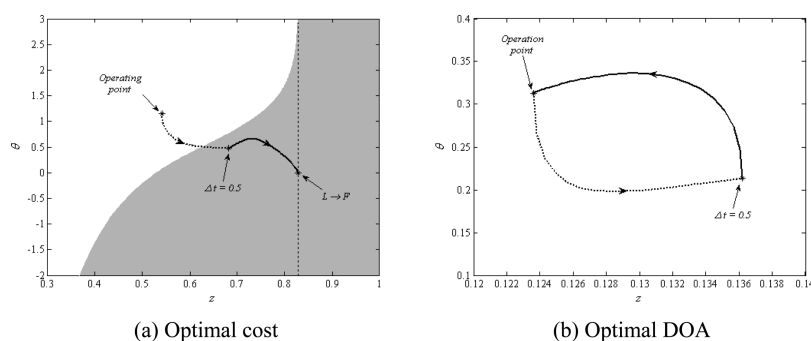


Figure 5. Dynamic simulation.

$\Delta t = 0.5$ (dotted arrow). Once the disturbance disappears, the initial condition of the system is outside the DOA of the original equilibrium and the system evolves toward a new operating condition (solid arrow). In the new situation the composition z approaches x_e , flow-rate V tends to zero and flow-rate L tends to flow-rate F . This very low production state is clearly undesirable from an operating point of view.

The optimal DOA counterpart (Figure 5b), on the other hand, presents a slight shift in the state space due to the step disturbance (dotted arrow). Once the disturbance disappears, the system returns to the previous equilibrium because the originated trajectory never left its DOA (solid arrow). Note that panels a and b in Figure 5 are in different scales for better resolution.

6. CONCLUSIONS

In this contribution, a design methodology based on the optimization of the domain of attraction has been applied to the design of a reactor–separator–recycle system. The idea is to simultaneously ensure asymptotic stability and an optimum domain of attraction of the resulting operating point in a certain sense. Specifically, the proposed merit function to be maximized was the radius of a ball in the states space within which negative definiteness of the time derivative of a quadratic type Lyapunov function can be ensured. Within such a ball it is possible to inscribe an invariant elliptic set which can be considered an estimation of the actual DOA of the equilibrium.

DOAs of stable equilibriums of nonlinear systems are usually complex shaped sets that can be hardly described precisely. However, the enlargement of the radius of the described ball has a “push away” effect on the actual boundaries of the DOA no matter their shape and localization. Such boundaries are usually the stable manifolds of saddle nodes. The enlargement of the DOA can be also achieved by a shift of the operating point in the state space.

From a mathematical point of view, the resulting is a bilevel optimization problem with nondifferentiable inner sub problems, in general. In order to address such potential nondifferentiability, a stochastic (derivative free) algorithm was adopted in the outer level to explore the design space.

To illustrate the proposed procedure, a RSRS was analyzed. In each case, the DOA optimized design was compared against a more classic cost optimized design under stability constraints. The typical conflicting trade-off between economics and operability was verified, since an enlarged DOA could be obtained at the expense of more expensive design.

From a physical point of view, the enlargement of the DOAs was achieved by working at low temperature and conversion levels. Because temperature has a large effect on the balances due to the exponential terms, it results evident that working at low temperatures provides larger “buffer zones” in the state space for the system to evolve under disturbances, before crossing “no return” points. This was demonstrated by dynamic simulation in the context of reaction runoff.

As future work, the application of the methodology to larger systems in the design and parameter spaces will be addressed. Although the methodology is general and not limited to small scale examples, the major limitation to address large scale models is the solution of the difficult inner optimization problem. Because global optimality is a must, expensive calculation is in general required for each function evaluation, hindering the efficient resolution of the design problem.

ACKNOWLEDGMENT

This work was partially supported by “Concejo Nacional de Investigaciones Científicas y Técnicas”, “Agencia Nacional de Promoción Científica y Técnica”, and “Universidad Nacional del Sur” of Argentina.

NOTATION

- A = Jacobian matrix
- A_{HX1} = heat exchange area exchanger 1 (m^2)
- A_{HX2} = heat exchange area exchanger 2 (m^2)
- A_r = heat transfer area of reactor (m^2)
- A_i = Antoine constant (Pa)
- B_i = Antoine constant (K)
- B = dimensionless heat of reaction (–)
- β = dimensionless heat transfer coefficient (–)
- β_{pay} = payback period (3 years)
- $C_{\text{exchangers}}$ = Capital cost of heat exchangers (\$/year)
- C_{reactor} = capital cost of reactor (\$/year)
- C_{flash} = capital cost of flash (\$/year)
- D_r = reactor diameter (m)
- D_{fl} = flash drum diameter (m)
- E = activation energy (J/mol)
- I = identity matrix
- C_{pm} = molar heat capacity (J/K/mol)
- D_a = Damköhler number
- F = reactor flow-rate (mol/s)
- F_0 = reactor feed flow-rate (mol/s)
- ϕ = cost objective function (\$/year)
- Δh_i = heat of vaporization (J/mol)

ΔH = heat of reaction (J/mol)
 k_0 = pre-exponential factor (mol/(m³ s))
 K_i = distribution constant (–)
 L = recycle flow-rate (mol/s)
 λ = eigenvalue
 M_r = reactor molar holdup (mol)
 P_{fl} = flash pressure (Pa)
 P_i = pure component saturation pressure (Pa)
 ρ_m = molar density (mol/m³)
 R = gas constant (J/(K mol))
 T = temperature (K)
 T_i = boiling point temperature (K)
 T_0 = reference temperature (K)
 T_a = refrigerant temperature (K)
 T_f = feed temperature (K)
 t = dimensionless time
 θ = dimensionless temperature
 U = heat transfer coefficient (J/(m² K))
 V_r = reactor volume (m³)
 V = flow rate of the vapor from the flash (mol/seg)
 x_e = mole fraction of reactant A in the liquid from the flash (–)
 x_{af} = mole fraction of reactant A in the feed (–)
 y_e = mole fraction of reactant A in the vapor from the flash (–)
 z = mole fraction of reactant A in the liquid from the mixing tank (–)

Subscripts

f = feed
 fl = flash
 i = component
 r = reactor
 HX1 = heat exchanger 1
 HX2 = heat exchanger 2

REFERENCES

- Luyben, W. L. Dynamics and Control of Recycle Systems. 1. Simple Open-Loop and Closed-Loop Systems. *Ind. Eng. Chem. Res.* **1993**, 32 (3), 466–475.
- Pushpavanam, S.; Kienle, A. Nonlinear Behavior of an Ideal Reactor Separator Network with Mass Recycle. *Chem. Eng. Sci.* **2001**, 56 (8), 2837–2849.
- Zeyer, K. P.; Kulkarni, A. A.; Kienle, A.; Kumara, M. V.; Pushpavanam, S. Nonlinear Behavior of Reactor-separator Networks: Influence of the Energy Balance Formulation. *Ind. Eng. Chem. Res.* **2007**, 46 (4), 1197–1207.
- Vetukuri, S. R. R.; Pushpavanam, S.; Zeyer, K. P.; Kienle, A. Nonlinear Behavior of Coupled Reactor-Separator Systems with Azeotropic Vapor-liquid Equilibria (VLEs): Comparison of Different Control Strategies. *Ind. Eng. Chem. Res.* **2006**, 45 (3), 1019–1028.
- Berger, J. S.; Perlmutter, D. D. Chemical Reactor Stability by Lyapunov's Direct Method. *AIChE J.* **1964**, 10 (2), 233–245.
- Pellegrini, L.; Biardi, G.; Grotto, M. G. Determination of the Region of Asymptotic Stability for a CSTR. *Comput. Chem. Eng.* **1988**, 12 (2–3), 237–241.
- Szederkényi, G.; Kristensen, N. R.; Hangos, K. M.; Jorgensen, S. B. Nonlinear Analysis and Control of a Continuous Fermentation Process. *Comput. Chem. Eng.* **2002**, 26, 659–670.
- Khalil, H. K. *Nonlinear Systems*; Prentice Hall: Upper Saddle River, NJ, 1996.
- Kokossis, A. C.; Floudas, C. A. Stability in Optimal Design: Synthesis of Complex Reactor Networks. *AIChE J.* **1994**, 40 (5), 849–861.
- Ringertz, U. T. Eigenvalues in Optimum Structural Design. In *Proceedings of an IMA Workshop on Large-Scale Optimization Part I*; Conn, A.R., Biegler, L.T., Coleman, T.F., Santosa, F., Eds.; Institute for Mathematics and Its Applications, University of Minnesota: Twin Cities, MN, 1997; pp 135–149.
- Monnigmann, M.; Marquardt, W. Steady-State Process Optimization with Guaranteed Robust Stability and Feasibility. *AIChE J.* **2003**, 49 (12), 3110–3126.
- Monnigmann, M.; Marquardt, W. Steady-State Process Optimization with Guaranteed Robust Stability and Flexibility: Application to HDA Reaction Section. *Ind. Eng. Chem. Res.* **2005**, 44 (8), 2737–2753.
- Gerhard, J. M.; Monnigmann, M.; Marquardt, W. Steady State Optimization with Guaranteed Stability of a Tryptophan Biosynthesis Model. *Comput. Chem. Eng.* **2008**, 32, 2914–2919.
- Blanco, A. M.; Bandoni, J. A. Eigenvalue Optimization-based Formulations for Nonlinear Dynamics and Control Problems. *Chem. Eng. Proc. Process Intensif.* **2007**, 46 (11), 1192–1199.
- Matallana, L. G.; Blanco, A. M.; Bandoni, J. A. Eigenvalue Optimization Techniques for Nonlinear Dynamic Analysis and Design. In *Optimization in Food Engineering*; Erdogdu, F., Ed.; Contemporary Food Engineering Series; Taylor and Francis Group: , 2008; Chapter 2.10, pp 271–293.
- Chang, Y.; Sahinidis, N. V. Optimization of Metabolic Pathways under Stability Considerations. *Comput. Chem. Eng.* **2005**, 29, 467–479.
- Lu, X.; Li, H.; Chen, C. L. P. Robust Optimal Design with Consideration of Robust Eigenvalue Assignment. *Ind. Eng. Chem. Res.* **2010**, 49 (7), 3306–3315.
- Genesio, R.; Tartaglia, M.; Vicino, A. On the Estimation of Asymptotic Stability Regions: State of the Art and New Proposals. *IEEE Trans. Autom. Control* **1985**, 30 (8), 747–755.
- Matallana, L. G.; Blanco, A. M.; Bandoni, J. A. Nonlinear Dynamic Systems Design Based on the Optimization of the Domain of Attraction. *Math. Comput. Modell.* **2010**, 53, 731–745.
- Vidyasagar, M. *Nonlinear Systems Analysis*; Prentice Hall: Upper Saddle River, NJ, 1993.
- Hahn, W. *Stability of Motion*; Springer-Verlag: New York, 1967.
- Matallana, L. G.; Blanco, A. M.; Bandoni, J. A. Estimation of Domains of Attraction: A Global Optimization Approach. *Math. Comput. Modell.* **2010**, 52, 574–585.
- Matlab, Mathworks. *Genetic algorithm and direct search toolbox*; The Mathworks Inc.: Natick, MA, 2004.
- GAMS: A Users' Guide; GAMS Development Corporation: Washington, D.C., 2008.
- GAMS: The Solvers Manual; GAMS Development Corporation: Washington, D.C., 2008.
- Tawarmalani, M.; Sahinidis, N. V. *Convexification and Global Optimization in Continuous and Mixed-Integer Nonlinear Programming: Theory, Algorithms, Software, and Applications*; Nonconvex Optimization and Its Applications; Kluwer Academic Publishers: Dordrecht, The Netherlands, 2002; Vol. 65.
- Strogatz, S. H. *Nonlinear Dynamics and Chaos*; Addison–Wesley Publishing Company: Boston, MA, 1994.
- Palazoglu, A.; Arkun, Y. A. Multiobjective Approach to Design Chemical Plants with Robust Dynamic Operability Characteristics. *Comput. Chem. Eng.* **1986**, 10 (6), 567–575.
- Bansal, V.; Perkins, J. D.; Pistikopoulos, E. N.; Ross, R.; van Schijndel, J. M. G. Simultaneous Design and Control Optimization Under Uncertainty. *Comput. Chem. Eng.* **2000**, 24, 261–266.
- Blanco, A. M.; Bandoni, J. A. Interaction between Process Design and Process Operability of Chemical Processes: An Eigenvalue Optimization Approach. *Comput. Chem. Eng.* **2003**, 27 (8–9), 1291–1301.
- Blanco, A. M.; Bandoni, J. A. Design for operability: A singular-value optimization approach within a multiple-objective framework. *Ind. Eng. Chem. Res.* **2003**, 42 (19), 4340–4347.